

# Coulomb-nuclear interference and isospin characterization of the first $2^+$ and $3^-$ transitions by inelastic scattering of alpha particles on $^{90,92}\text{Zr}$

*L. B. Horodynski-Matsushigue, T. Borello-Lewin, M. R. D. Rodrigues, C. L. Rodrigues, H. Miyake*

Instituto de Física, Universidade de São Paulo, São Paulo, Brasil

## Abstract

Angular distributions for inelastic scattering of 21 MeV alpha particles, exciting the first  $2^+$  and  $3^-$  states of  $^{90,92}\text{Zr}$ , were measured using the São Paulo Pelletron-Enge-Spectrograph facility. Coulomb-nuclear interference analysis was applied and values of  $C_L = \delta_L^C / \delta_L^N$ , the ratios of charge to isoscalar deformation lengths for  $L=2(3)$  and of  $\delta_L^N$  were extracted, through comparison of experimental cross sections to DWBA-DOMP predictions. A relative accuracy of  $\sim 5\%$  was achieved for  $C_L$ . The ratio of reduced charge to isoscalar transition probability,  $B(\text{EL})$  to  $B(\text{ISL})$ , is, for each  $L$ , related to the square of the parameter  $C_L$ . A homogeneous collective excitation was revealed by  $C_2 = 1.057(50)$  for the first  $^{90}\text{Zr}$  quadrupole transition, in sharp contrast with the  $C_2 = 0.587(20)$  value extracted for  $^{92}\text{Zr}$ . No such difference was detected for the octupole excitations, since values of  $0.865(47)$  and  $0.870(37)$   $C_3$  were determined for  $^{90}\text{Zr}$  and  $^{92}\text{Zr}$ , respectively. A strong  $^{92}\text{Zr}$  GS configuration mixing is suggested.

## 1 Introduction

The Zirconium isotopic chain, where rather abrupt changes in nuclear properties are experimentally observed, in special along the region of  $N$  from 50 to 60, has attracted renewed interest in recent years. In particular, a group of authors of the University of Tokyo [1], after performing large-scale Monte Carlo shell model calculations, claims that a “Quantum Phase Transition” is observed in the systematics of the excitation energies of low-lying states in Zr isotopes. Shape coexistence has consistently been invoked as a cause of some of the experimentally observed aspects and the work of Heyde and Wood [2] may be taken as an example. However, from an experimental point of view, several unexpected results continue to intrigue researchers, resulting in an effort to find causes for differences in the outcomes of inelastic scattering by different probes, either in the data themselves or in their analyses.

Some years ago, a great investment was made in the attempt of reconciling results of a ( $^6\text{Li}, ^6\text{Li}'$ ) work on Zr isotopes obtained by the Yale group [3] with other data, particularly with findings of a former ( $\alpha, \alpha'$ ) experiment on  $^{90-96}\text{Zr}$ , performed in Heidelberg by Rychel et al. [4]. With this purpose, a very careful reproduction of the Heidelberg alpha scattering experiment was undertaken by Lund et al. [5], at the Yale facility, with the same incident energy of 35.4 MeV. No disagreement with the German data or their analysis was found. In fact, a clear explanation of the observed results is still lacking.

In this scenario, it is the purpose of the present work to put forward some interesting aspects of experimental studies which examine differences between  $^{90}\text{Zr}$  and its neighbours, as part of a study program aiming at collective properties in the Zr-Mo-Ru region, using light  $T=0$  projectiles at the São Paulo Pelletron-Enge-Spectrograph facility. The unpublished data for  $^{90,92}\text{Zr}$  ( $\alpha, \alpha'$ ) [6], are being analysed in more detail, in view of recent interpretations. Coulomb-nuclear interference (CNI) effects are much enhanced at the lower incident energy of 21 MeV chosen in this experiment, which favours the isospin characterization of the transitions to the first  $2^+$  and  $3^-$  states.

## 2 Experimental Setup

The São Paulo Pelletron-Enge-Spectrograph system has been employed in several high resolution studies of isotopic chains in the  $A \sim 100$  region, due to its excellent energy resolution. Special care was taken in the present work to optimize resolution and accuracy of the Zr data. Two kinds of targets were produced in the Target Laboratory at the S. Paulo Pelletron facility in order to optimize experimental conditions. Being essential for good forward-angles measurements, rectangular spot targets were fabricated for both Zr isotopes ( $A=90,92$ ) to guarantee an adequate object for the spectrograph while avoiding scattering on defining slits, which could be maintained wide open. Furthermore, as an important factor to obtain good quality spectra at intermediate scattering angles, self-supported thin targets of the same isotopes were also produced. These were employed to increase substantially the Zr to C and O rates, allowing those light contaminants, which are associated with wide unfocused peaks on the detection plane, to be better separated from the peaks of interest.

The emerging ions of the reaction, admitted and momentum analysed by the field of the spectrograph, were detected on the focal surface either by nuclear emulsion plates (Fuji G6B 50 micron thick, covering 25cm) or by a position sensitive 38cm gas detector [7]. The detector was basically a combination of a drift chamber and a proportional counter with a cylindrical delay line providing the position information. More than forty spectra were measured at carefully chosen scattering angles in a range of  $14^\circ \leq \theta_{\text{Lab}} \leq 80^\circ$  in order to characterize CNI in the angular distributions corresponding to the first quadrupole and octupole excitations in both nuclei. An overall energy resolution between 17 and 22 keV was achieved using a spectrograph entrance solid angle of 2.68 msr. Relative normalization of the data for the various scattering angles was obtained through simultaneous measurements of elastic scattering, while, for absolute normalization, optical model predictions to experimental elastic data, on the same target and under similar conditions, were considered. The absolute uncertainty of the experiment is estimated to be 20%.

## 3 Data analysis and Results

To extract relative transition probabilities between the ground state and the excited levels of interest, the distorted wave Born approximation (DWBA) prediction employing the deformed optical potential model (DOMP) approach was applied to the experimental angular distributions. The effective transition potential responsible for nuclear excitation is associated with non-sphericities of the optical potential, whether these are of dynamic or static origin. An adequate parametrization of the intensity of macroscopic effects is thus provided. In the present work, the same geometry and deformation lengths for the real and imaginary parts of the standard Woods-Saxon optical potential employed by Rychel et al. [4], for  $\alpha$  particles of 35.4 MeV, were taken. Incident energy corrections of the corresponding well depths, following Put and Paans in their extensive work on an optical model for alpha particles [8], were applied. The total transition potential is the sum of Coulomb and nuclear transition potentials. The corresponding Coulomb transition potential for radii ( $r$ ) equal or larger than  $R_C$  determines the reduced electric transition probability  $B(EL)$  [5]. In the present work, for  $r$  smaller than  $R_C$  the Coulomb transition potential is taken to be zero without harm, since the reaction occurs peripherally.

The values of the ratio,  $C_L$ , between the charge,  $\delta_L^C$ , and mass,  $\delta_L^N$ , deformation lengths for  $L=2(3)$  were obtained from the best fits to the shapes of the angular distributions associated, respectively, with the  $2^+$  and  $3^-$  excitations in both nuclei. The square of the corresponding mass deformation lengths,  $(\delta_L^N)^2$  was also extracted, as a scale factor. The procedure applied for the  $\chi^2$  minimization was the iterative method of Gauss, extracting the correlated parameters  $\delta_L^N$  and  $C_L$ . The ratio  $B(EL)/[B(ISL)e^2]$ , considering the definition of  $B(ISL)$  scaled by  $Z$ , as proposed by Bernstein et al. [9], is expressed by the product of the squares of  $C_L$  and  $(r_o^c / r_o^m)^{L-1}$  and is also obtained. In the present work, the values of  $r_o^c = 1.22$  fm and  $r_o^m = 1.16$  fm for, respectively, the charge and the mass reduced nuclear radii sharp cut-off distributions were used.

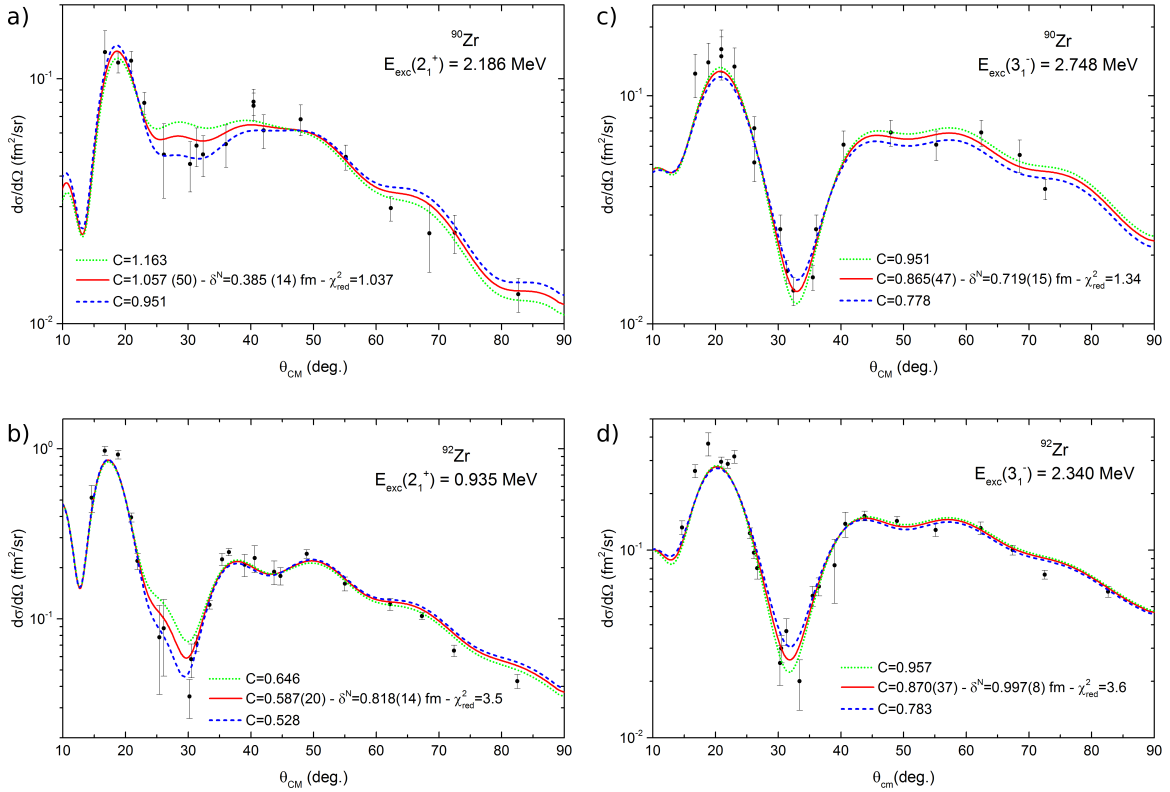


**Fig. 1:** Comparison of experimental angular distributions with DWBA-DOMP predictions for inelastic alpha scattering on  $^{90,92}\text{Zr}$ , exciting the first quadrupole and octupole levels. Full lines represent the best fit and correspond to indicated values of the correlated parameters ( $C$  and  $\delta^N$ ), while respectively, dotted(interrupted) ones represent fits with values of the  $C$  parameter increased(decreased) by two (or, exceptionally, three) times the attributed uncertainties.

Figures 1(a)-(d) illustrate the results obtained from the best fit of the experimental angular distributions for  $^{90,92}\text{Zr}(\alpha, \alpha')$  in the excitation of the first quadrupole ( $L=2$ ) and octupole ( $L=3$ ) excited states, when compared to DWBA-DOMP predictions, in each nucleus. The error bars represent the relative uncertainties composed by the statistical uncertainties and the contribution from the background and contaminant subtraction. The results obtained in this data analysis for the two correlated parameters of interest, the corresponding random uncertainties and reduced  $\chi^2$ , are also indicated. It is to be noted, however, that the absolute scale uncertainty was incorporated in the final results. For  $^{90}\text{Zr}$ , the best fits for, respectively,  $L=2$  and  $L=3$ , are shown in Figs. 1(a) and (c), while the fits corresponding to  $^{92}\text{Zr}$  are presented in Figs. 1(b) and (d). The values extracted for  $C$  and  $\delta^N$  are given in each of the respective figures. In order to illustrate the sensibility of the method, the predicted angular distributions associated with values of  $C$  corresponding, respectively, to that of the best fit (continuous curve) and this value increased (dotted curve) and decreased (interrupted curve), by about two times the calculated random uncertainty, are also presented, in each figure.

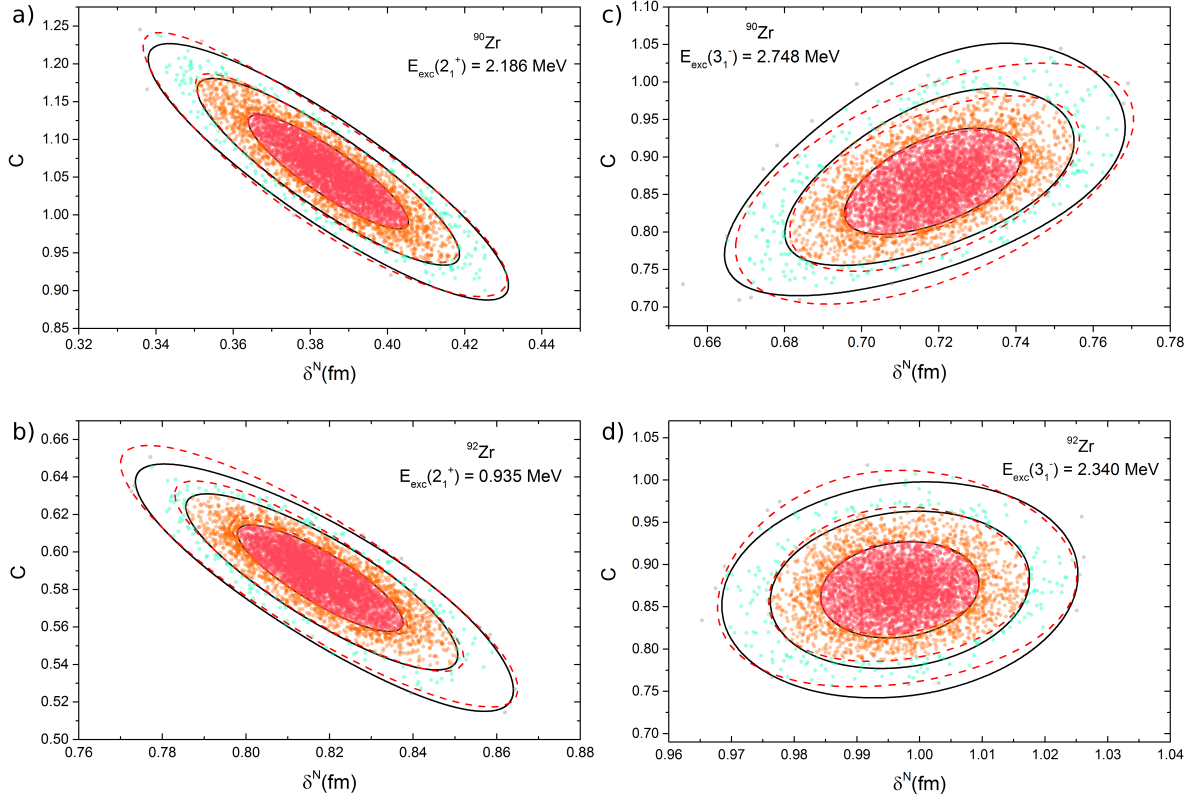


**Fig. 2:** Results from Monte Carlo simulations for the first quadrupole and octupole excitations in  $^{90,92}\text{Zr}$ . Also shown are the contour lines CL (full lines) and Gauss ellipses GE (interrupted lines), respectively, associated with usual 68.3%, 95.5% and 99.7% confidence levels. The adequacy of the attributed uncertainties in the extracted parameters may, thus, be appreciated.

A Monte Carlo (MC) simulation of 5000 angular distributions, each one generated by randomly choosing values from a Gaussian distribution with the given standard deviation around each experimental point, was used to illustrate the adequacy of the attributed uncertainties. In fact, almost elliptical  $\chi^2$  contour lines (CL) associated with usual confidence levels (68.3%, 95.5% and 99.7%) were obtained. Figures 2(a) and (b) show the MC results for the  $^{90,92}\text{Zr}$   $2^+_{11}$  excitations, respectively, and the CL associated with the indicated confidence levels (full lines). For comparison, the Gauss approximation ellipses (GE) (interrupted lines), corresponding to the same confidence levels, are also presented. Figs. 2(c) and (d) show the results for the  $^{90,92}\text{Zr}$   $3^-_{11}$  excitations. For the first quadrupole excitations, in both nuclei, the resulting contour lines (CL) agree very well with the Gauss ellipses (GE). The corresponding results for octupole excitations reveal CL which also follow the GE, but with slightly higher deviations.

The final results obtained in this work are:  $C_L$ ,  $\delta_L^N$  and  $B(\text{EL})/[B(\text{ISL})e^2]$ , associated with the first quadrupole ( $L=2$ ) and octupole ( $L=3$ ) excitations for  $^{90}\text{Zr}$  and  $^{92}\text{Zr}$ , as shown in Table 1.

It is to be noted that the ratios  $B(\text{EL})/[B(\text{ISL})e^2]$  here determined were not previously reported and to be stressed that these ratios are not affected by the scale uncertainty.

**Table 1:** Results for first quadrupole and octupole excitations by inelastic alpha scattering on  $^{90,92}\text{Zr}$ 

A	$C_2$	$\delta_2^N$ (fm)	B(E2)/B(IS2) ( $e^2$ )	$C_3$	$\delta_3^N$ (fm)	B(E3)/B(IS3) ( $e^2$ )
90	1.057(50)	0.385(42)	1.24(12)	0.865(47)	0.719(72)	0.91(10)
92	0.587(20)	0.817(82)	0.381(27)	0.870(37)	0.997(99)	0.93(8)

Table 1 shows a strongly depressed  $C_2$  value for the first quadrupole excitation in  $^{92}\text{Zr}$ , in comparison with the almost homogeneous excitation in  $^{90}\text{Zr}$ . Due to the cancellation of scale uncertainties in this ratio, the experimental values of  $B(E2)/[B(IS2)e^2]$ , here presented for the first time, were obtained with a relative accuracy of 10% and 7%, for  $^{90}\text{Zr}$  and  $^{92}\text{Zr}$ , respectively.

In contrast, the present investigation points to very similar values for the first octupole collective excitations in both,  $^{90,92}\text{Zr}$ , these being practically homogeneous, since only a very slight predominance of the neutrons relative to the protons has been detected. The experimental ratios  $B(E3)/[B(IS3)e^2]$  which also had not been previously reported, were extracted with a relative accuracy of 11% and 9%, for  $^{90,92}\text{Zr}$ , respectively.

The very complete work of Lund et al. [5], presenting much more detailed data than did Rychel et al. [4] could not define the CNI region as well as the present experiment, since performed at the higher incident alpha particles energy of 35.4MeV. The  $\delta_L^N$  values, here extracted agree with the values of the DOMP analysis reported in Ref. [5], for both states,  $2^+$  and  $3^-$ , in  $^{90,92}\text{Zr}$ .

It is to be noted that inelastic scattering, even if there is configuration mixing in the ground state, would excite only the configuration that connects the ground and the  $2^+_1$  states of each isotope. In this context, the  $C_2$  value extracted for  $^{92}\text{Zr}$  suggests a strong ground state configuration mixing involving not only the neutron degree of freedom, but also probably other configurations associated with subshell closures. These configurations, in the neighbourhood, are possibly an alpha or (2p+2n) plus a core of  $^{88}\text{Sr}$  ( $Z=38$ ,  $N=50$ ) [10] and (2n) plus  $^{90}\text{Zr}$  ( $Z=40$ ,  $N=50$ ).

The  $C_2$  values extracted in this CNI study for the first quadrupole excitations in  $^{90,92}\text{Zr}$  reveal a clear difference in the contribution of protons relative to the neutrons in those neighbouring isotopes. In  $^{92}\text{Zr}$  the neutron role is strongly enhanced to an extent not formerly observed in other nuclei and represents an abrupt change in comparison with  $^{90}\text{Zr}$ , for which the measured value indicates a homogeneous excitation.

### Acknowledgements

T.B.L, M.R.D.R. and H.M. are members of INCT-FNA, Brazil

### References

- [1] T. Togashi, Y. Tsunoda, T. Otsuka and N. Shimizu, *Phys. Rev. Lett.* **117**, 172502 (2016).
- [2] K. Heyde and J. L. Wood, *Rev. Mod. Phys.* **83**(2011) 1467.
- [3] D. J. Horen et al., *Phys. Rev.* **C47**(1993) 629.
- [4] D. Rychel et al., *Z. Phys.* **A326**(1987) 455.
- [5] B. J. Lund et al., *Phys. Rev.* **C51**(1995) 635.
- [6] L. B. Horodyski-Matsushigue, T. Borello-Lewin and J. L. M. Duarte, *Int. Nucl. Phys. Conf.*, São Paulo Brasil 1989, Proceedings **I**, 307.
- [7] K. Koide et al., *Nucl. Instrum. and Meth.* **215** (1983) 177.
- [8] L. W. Put and A. M. J. Paans, *Nucl. Phys.* **A291**(1977) 93.
- [9] A. M. Bernstein, V. R. Brown and V. A. Matser, *Phys. Lett.* **B71**(1977) 48, **B103** (1981) 255.
- [10] M. A. Souza, H. Miyake, *Phys.Rev.* **C91**, 034320 (2015).

